J. Fluid Mech. (1965), *vol.* 22, *part* 2, *pp.* 321–335
Printed in Great Britain

The investigation of a standing wave due to gas blowing upwards over a liquid film; its relation to flooding in wetted-wall columns

By C. J. SHEARER† AND J. F. DAVIDSON
Department of Chemical Engineering, University of Cambridge

(Received 8 January 1964 and in revised form 12 November 1964)

A theory is given to predict the shape and amplitude of a standing wave formed on a liquid film running down a vertical surface, and due to an upward flow of gas over the liquid surface. The wave is maintained in position by the pressure gradients induced within the gas stream by acceleration over the windward part of the wave; over the leeward part of the wave, the gas pressure is roughly constant due to breakaway of the gas flow.

The wave amplitude is found to be very sensitive to gas velocity so that the theory predicts a critical gas velocity beyond which the wave amplitude becomes very large; this critical velocity is confirmed by experiment, and the experiments confirm the predicted wave shape. The critical gas velocity also agrees reasonably well with published values of the flooding velocity in empty wetted-wall tubes; this velocity is defined as the point at which countercurrent flow of gas and liquid becomes unstable. The phenomenon of flooding, which has puzzled chemical engineers for many years, may thus be due to wave formation on the liquid film.

From the theory are derived three dimensionless groups, namely, Weber number $We \equiv \rho_g U_c^2 t_0/T$, liquid-film Reynolds number $Re \equiv 4\rho_l Q/\mu$, and $Z \equiv T(\rho_l/\mu g)^{\frac{1}{3}}/\mu$. Here U_c is the critical gas velocity, Q is the liquid volume flow rate per unit wetted perimeter, ρ_g and ρ_l are the gas and liquid densities, μ is the liquid viscosity and T is its surface tension; $t_0 = (3\mu Q/\rho_l g)^{\frac{1}{3}}$ is the liquid film thickness in the absence of gas flow. *We*, *Re* and Z are uniquely related at the flooding point, and a diagram is presented to show this relation. This diagram will enable designers to predict flooding in wetted-wall tubes, though more experimental verification is required.

1. Introduction

A wetted wall column is a device used in the laboratory by chemical engineers for contacting a gas with a liquid; the apparatus consists of a vertical tube with a thin film of the liquid running freely under gravity down the inside wall, the gas being blown upwards through the tube, thus giving reasonably well-defined conditions of contact between the two phases. One problem that immediately arises is to find, at a given liquid rate, the maximum gas flow beyond which the countercurrent flow will not persist, some of the liquid being carried up by the

† Present address: Shell Development Company, Emeryville, California.

gas stream. Experiments show that this limiting gas flow, the flooding velocity, can be measured with reasonable precision; the present paper gives a theory to predict it.

The basis of our theory is to assume that, at the limiting gas flow, a standing wave forms on the liquid surface, the amplitude being several times the mean film thickness. The calculations show that the wave amplitude is very sensitive to gas flow so that within a narrow range of increasing flows, the amplitude becomes very large indeed, and the upper limit of this range agrees with the measured gas flow for flooding of the wetted-wall column.

The study of standing waves began with a rather different problem considered by Davidson & Howkins (1957). Their problem was the instability of a vertical water film due to pressure gradients within air accelerating upwards over the water surface. They studied the small amplitude instability of the film, and incidentally found that a large wave, having an amplitude many times the mean film thickness, could be formed; it is *this* wave with which we are now concerned. Experiments with Davidson & Howkins' apparatus established the shape of the wave, shown in figure 2, plate 1, and it was possible to develop a theory to predict this shape. It was then clear that the pressure gradients necessary for Davidson & Howkins' small amplitude instability are unimportant in the wave shown in figure 2. This wave is supported by pressure gradients within the air stream on the windward side; but these pressure gradients are *due to the wave itself*, whereas in Davidson & Howkins' problem, the pressure gradients were imposed by making the air accelerate through a nozzle. Also, for the wave shown in figure 2, the air flow breaks away above the crest; in Davidson & Howkins' theory there was no such breakaway.

Having established that the wave shown in figure 2 could occur with a uniform upward flow of air over a water film, it seemed likely that such a wave might be formed in wetted wall columns. That such waves are the cause of flooding is indicated by the fact that experimental data on flooding agree quite well with theory based on the calculations for the wave shown in figure 2.

2. Experiment

Figure 1 is a diagram of the apparatus, which was the same as that of Davidson & Howkins (1957) with the following modifications:

(*a*) their 1 in. diameter brass tube was replaced by a Perspex rod; and

(*b*) the orifice plate AA was as shown in figure 1 with the chamfer on the lower side, instead of the upper side as used by Davidson & Howkins.

Both of these modifications made it easier to see the wave; in other respects the apparatus was the same as that of Davidson & Howkins who described it in detail.

Wave formation

Figure 2 shows the wave that could be formed just above the orifice AA in figure 1. The wave was stable within only a very narrow range of air and water rates around the values shown in figure 2. If the air rate was decreased slightly, the wave disappeared altogether; if the air rate was increased, droplets were

ripped off the crest of the wave. If the water rate was reduced, the tube did not wet properly, and if it was increased, there was much rippling and this made the wave unstable.

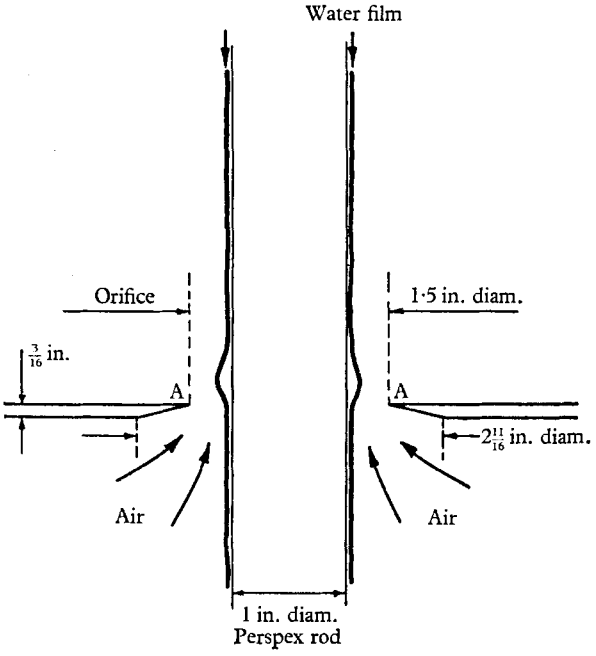

FIGURE 1. Diagrammatic representation of the apparatus.

Pressure distribution over the wave

Measurements of pressure distribution over solid models of a single wave, and of a wave train, have been summarized by Ursell (1956), who described several investigations of this kind. None of these is directly applicable to the present problem, because our wave has a much greater ratio of amplitude to wavelength than in the studies described by Ursell who dealt with waves due to wind.

Figure 2 is a direct photograph of the wave, and the wave profile seen in the photograph was copied in brass by turning on a lathe two brass sections 8 in. long and initially of semi-circular cross-section. The two halves were temporarily bonded together along a diametral plane, and when the wave profile had been turned, a 0·75 in. diameter hole was bored along the axis of the assembly. This was then separated, and pressure tapping holes 0·0165 in. in diameter were drilled normal to the wave surface; from each hole a lead of stainless-steel hypodermic tubing was then soldered in position, and the two halves were bonded together again. The assembly was then substituted for the Perspex tube in the apparatus of figure 1, the brass wave being in the same position as the water wave had been. Air was then passed through at the rate for wave formation, and the pressure at each tapping measured with a Chattock gauge, giving the experimental pressure distribution shown in figure 3. This shows clearly the drop in pressure due to acceleration of the air over the wave, with partial pressure recovery on the leeward side of the crest, and subsequent breakaway over the main part of the

lee-side of the wave. Reattachment of the air flow seems to take place at about the point where the wave ends, that is, where the liquid film becomes uniform in thickness above the wave.

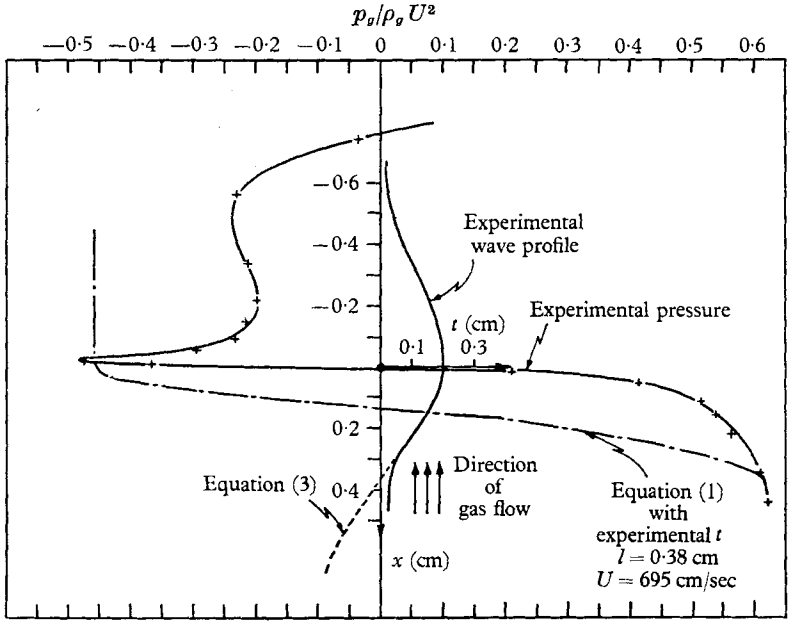

FIGURE 3. Pressure distribution over standing wave.

3. Theory of the standing wave

The theory depends upon the assumption that the gas flow breaks away at the crest of the wave, so that there is a constant pressure in the gas on the leeward side and varying pressure due to acceleration of the gas on the windward side; the varying pressure supports the wave. Within the liquid film, the wave shape on the leeward side is determined by a balance between gravity and surface tension forces, viscous and inertia forces being neglected. In calculating the wave shape on the windward side, gravity, surface tension, viscous, and inertia forces in the liquid film are allowed for, as well as the variation of pressure transmitted from the gas to the liquid phase.

All the assumptions are set out in detail below. The flow patterns on the gas and liquid sides are interdependent, but each can be considered separately.

Gas side

The forces exerted on the wave by the gas are calculated as follows.

(*a*) It will be assumed that the gas flow breaks away from the liquid surface on the leeward side of the wave, and hence in this region the gas pressure must be constant. This assumption is substantiated by the experimental pressure profile shown in figure 3, which indicates breakaway just behind the wave crest, with roughly constant pressure thereafter.

(*b*) We shall neglect the shear stress exerted on the liquid surface by the gas. An order-of-magnitude calculation shows that the effect of shear stresses on the

film is much less than the effect of normal pressure. Also, this assumption is partly justified by the experimental results of Nicklin & Davidson (1962); they found that up to the flooding point, the liquid film thickness in a wetted-wall tube is unaffected by the gas flow, showing that the effect of interfacial shear on the liquid film is small.

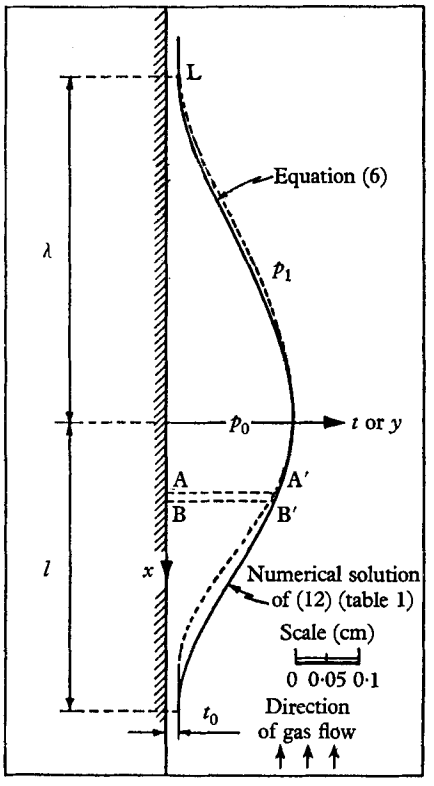

FIGURE 4. Axes and wave profiles to scale. The experimental profile from figure 2 is shown as broken line.

(*c*) For the variation of gas pressure over the windward surface of the wave we use the empirical expression

$$(P-p_g)/\rho_g U^2 = (\pi t/2l)\,(1+\pi t/4l). \tag{1}$$

Here P is the pressure far upwind from the wave, and p_g is the pressure at any point on its windward surface where the film thickness is t. The length l from the crest to the trough along the x-axis is indicated in figure 4, and U is the velocity of the gas stream.

Equation (1) is similar in form to the theoretical result given by Lamb (1932) for two-dimensional potential flow of two fluids parallel to their interface which has sinusoidal undulations of small amplitude. Neglecting second-order terms, the theory given by Lamb leads to

$$(P-p_g)/\rho_g U^2 = \pi t/2l, \tag{2}$$

the equation for the solid boundary being

$$t = -a \sin [\pi(x-l)/2l], \tag{3}$$

where a is the amplitude of the undulations.

Figure 3 shows (1) plotted by substituting values of t from the experimental profile. Equation (1) is seen to give a good estimate of the overall pressure drop from crest to trough; also, the pressure gradients are in fair agreement with measured values. Figure 3 also shows (3) plotted for comparison with the experimental profile; the two curves agree quite well for $0 < x < 0{\cdot}25$ cm.

Liquid side

Within the liquid film in the region λ in figure 4, viscous and inertia forces will be neglected; this approximation will be more valid in the thicker parts of the film near the wave crest; obviously viscous and possibly inertia forces are important in the thinner parts of the film. However, using this approximation throughout the region λ in figure 4 we infer that the pressure within the liquid must vary linearly with height. The gas pressure being constant within this region, in view of assumption (*a*) above, we have.

$$p_1 - p_0 - \rho_l g x = T(d^2t/dx^2), \tag{4}$$

p_0 being the liquid pressure just under the wave crest, and p_1 the gas pressure on the leeward side of the wave; ρ_l is the liquid density, g the acceleration due to gravity, T the surface tension, and x is the vertical co-ordinate shown in figure 4.

The boundary conditions for (4) at $x = 0$ are $t = a + t_0$ and $dt/dx = 0$, a being the wave amplitude. By integrating (4), using these boundary conditions to eliminate the constants of integration, and using also the conditions $t = t_0$, $dt/dx = 0$ at $x = -\lambda$, we get

$$p_0 - p_1 = \tfrac{1}{2}\rho_l g\lambda = (3aT\rho_l^2 g^2/2)^{\frac{1}{3}}, \tag{5}$$

$$t = a + t_0 - \left[\frac{3a}{2}\left(\frac{\rho_l g}{T}\right)^2\right]^{\frac{1}{3}} \frac{x^2}{2} - \frac{\rho_l g}{6T} x^3. \tag{6}$$

The wave amplitude a is an independent variable in the above analysis, and figure 4 shows that if a is chosen to have the experimental value, (6) gives a good prediction of the wave shape upwind from the crest. From (5) the pressure at L, figure 4, is $p_1 - \frac{1}{2}\rho_l g\lambda$. The actual pressure at L is probably higher, on account of viscous and inertia forces within the wave, and these forces must make the pressure equal to p_1 within the liquid a short distance above L, assuming that the gas pressure remains constant above L. But the experimental pressure distribution in figure 3 shows that reattachment of the gas flow occurs just above L, and this is a further complication. However, the neglect of viscosity and inertia within the liquid clearly gives almost the right wave shape though perhaps the wrong liquid pressure in the region above the crest.

Below the crest, viscous and inertia forces within the liquid will be included. These forces become dominant in the lowest part of the wave where the film thickness is approaching its asymptotic value.

We consider, therefore, the forces acting on the liquid between two fixed horizontal planes AA′ and BB′ with co-ordinates x, $x+dx$ as shown in figure 4. The downward resultant of the forces on the liquid between these planes must be $\rho_l g t\,dx-(dp_l/dx)\,t\,dx-\tau_w\,dx$, where τ_w is the wall shear stress at AB; we are assuming uniform pressure across a horizontal section, and as before, we are neglecting the interfacial shear stress at A′B′. The resultant force on the liquid must equal the net rate of transfer of momentum across the boundary AA′ BB′, and hence

$$\rho_l g t - t\frac{dp_l}{dx} - \tau_w = \frac{d}{dx}\int_0^t \rho_l v^2\,dy, \tag{7}$$

where v is the downward velocity of the liquid at any point within the film. The flow within the liquid is assumed to be laminar and $\tau_w = \mu(dv/dy)_{y=0}$, μ being the liquid viscosity; as a first approximation the velocity distribution is assumed to be parabolic, and therefore

$$v = \frac{\tau_w}{\mu}\left(y-\frac{y^2}{2t}\right). \tag{8}$$

This assumption is almost certainly wrong in the region of the wave crest, but in that region the viscous and inertia forces are small. However, the parabolic distribution must hold good far below the wave, where the film thickness

$$t_0 = (3\mu Q/\rho_l g)^{\frac{1}{3}}, \tag{9}$$

Q being the volume flow rate per unit width; in the region where $x \to l$, with which we are chiefly concerned, the parabolic distribution is likely to be a reasonable approximation. The total flow in the liquid film is $Q = \int_0^t v\,dy$, and substituting for v from (8) gives the relation

$$Q = \tau_w t^2/3\mu \tag{10}$$

between Q and τ_w. Finally, the gas and liquid pressures are related by

$$p_g - p_l = T(d^2t/dx^2), \tag{11}$$

p_g being given by (1), and we can then get the following differential equation for the film thickness t by eliminating p_l, p_g, v and τ_w from (1), (7), (8), (10) and (11) to give

$$T\frac{d^3t}{dx^3} + \frac{\pi\rho_g U^2}{2l}\left(1+\frac{\pi t}{2l}\right)\frac{dt}{dx} + \rho_l g + \frac{6}{5}\frac{\rho_l Q^2}{t^3}\frac{dt}{dx} - \frac{3\mu Q}{t^3} = 0. \tag{12}$$

The last two terms in (12) represent the effects of momentum and wall shear on the liquid film, and the second term in (12) represents the effect of pressure gradients in the gas stream.

Boundary conditions for t at $x = 0$

At the wave crest, $x = 0$, we must have

$$t = a + t_0, \quad dt/dx = 0. \tag{13}$$

A third boundary condition comes from the requirement that the pressure within the liquid just above and below the crest must be equal to p_0, and the gas pressure

must also be the same on either side of the crest; hence from (11) d^2t/dx^2 must be continuous through the crest. Therefore the third boundary condition for integration of (12) is obtained from (6) with $x = 0$,

$$(d^2t/dx^2)_{x=0} = -[\tfrac{3}{2}a(\rho_l g/T')^2]^{\frac{1}{3}}. \tag{14}$$

Integration of (12)

Equation (12) was solved by numerical integration using the method based on Taylor's series, as expounded by Jeffreys & Jeffreys (1946). The calculations were done by an I.B.M. 1620 digital computer with integration steps of 0·01 cm, and using the standard procedure for a 'marching' problem, as follows.

(*a*) The calculation began at $x = 0$ with assumed values of the amplitude a and length l, and proceeded from the boundary conditions (13) and (14), using (12) to trace out t as a function of x in the region below the wave crest.

(*b*) When dt/dx became zero, at the trough of the wave, the computer compared the film thickness t_l with the known asymptotic film thickness t_0 from (9).

(*c*) The value of x at the trough was used as a revised estimate of l to recalculate the coefficients in (12).

(*d*) The assumed amplitude a was then altered proportionately to the deviation $t_l - t_0$ at the trough and the cycle of calculations was repeated.

(*e*) When repeated cycles of the calculation gave a negligible deviation $t_l - t_0$ at the trough, the computer printed out the resulting wave form, and thus gave the wave amplitude and shape uniquely, for the given gas and liquid rates.

4. Results and comparison with the authors' experiments

Table 1 shows a typical set of values of film thickness t as a function of x, which satisfy (12), the boundary conditions (13) and (14), and give $t = t_0$ when $dt/dx = 0$. At a given gas velocity, the wave is thus completely determinate, and its shape is plotted in figure 4, the values in table 1 having been chosen to give the same wave amplitude as was measured experimentally from figure 2 at the same liquid Reynolds number. Figure 4 shows the good agreement that is obtained between the theoretical and experimental wave shapes, and this is perhaps the best verification of the theory. The agreement between the experimental and theoretical values of U, 695 and 926 cm/sec at the same wave amplitude, is poor. However, the experimental value of U is the volumetric air flow rate divided by the annular area between the orifice AA and the liquid film in figure 1; the actual velocity over the wave is probably somewhat higher than 695 cm/sec owing to the effect of the contraction coefficient of the sharp-edged orifice AA.

Figure 5 shows a series of calculated wave shapes [from (6) and (12)], at constant liquid rate and varying gas rate. The diagram demonstrates the extreme sensitivity of wave shape to gas rate; it is clear that the wave should be stable for only a very narrow range of gas flow rates, and this was certainly true for our apparatus. Figure 5 refers to a higher Reynolds number than the experimental one because at the lower value, the wave amplitude was so extremely sensitive to gas flow that is was very hard to get more than two wave shapes.

Figure 6 shows the wave amplitude, calculated from the above theory, plotted

as a function of the group $\rho_g U^2/\rho_l g$, with various values of the liquid flow rate, surface tension and viscosity; the particular values are those for which experimental data, to be described later, are available in the literature. Figure 6 shows

Fixed parameters: $T = 72{\cdot}5$ dyn/cm; $\rho_l = 1$ g/c.c.; $\mu = 1$ cP; $\rho_g = 0{\cdot}00122$ g/c.c.
Flow parameters: $U = 926$ cm/sec; $Q = 0{\cdot}25$ cm^2/sec; $t_0 = 0{\cdot}0198$ cm.
Step size: 0·01 cm.

x (cm)	t (cm)	x (cm)	t (cm)
0	0·1998	0·25	0·09842
0·05	0·1950	0·30	0·06946
0·10	0·1805	0·35	0·04526
0·15	0·1576	0·40	0·02813
0·20	0·1290	0·45	0·01983

TABLE 1. Typical computed wave-form

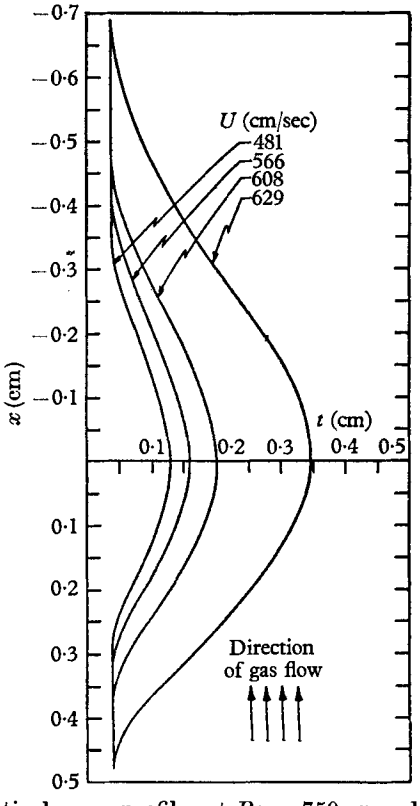

FIGURE 5. Theoretical wave profiles at $Re = 750$; $\mu = 1$ cP; $\rho_l = 1$ g/c.c.; $T = 72$ dyn/cm; $\rho_g = 0{\cdot}00122$ g/c.c.

how wave amplitude increases sharply with gas velocity, and there appears to be a critical value, U_c, beyond which the wave amplitude becomes very large. The variable $\rho_g U_c^2$ should be a function of Q, ρ_l, μ, T, g, and from (12), or from the theory of dimensionless groups, $\rho_g U_c^2 t_0/T = We$ the Weber number, should be

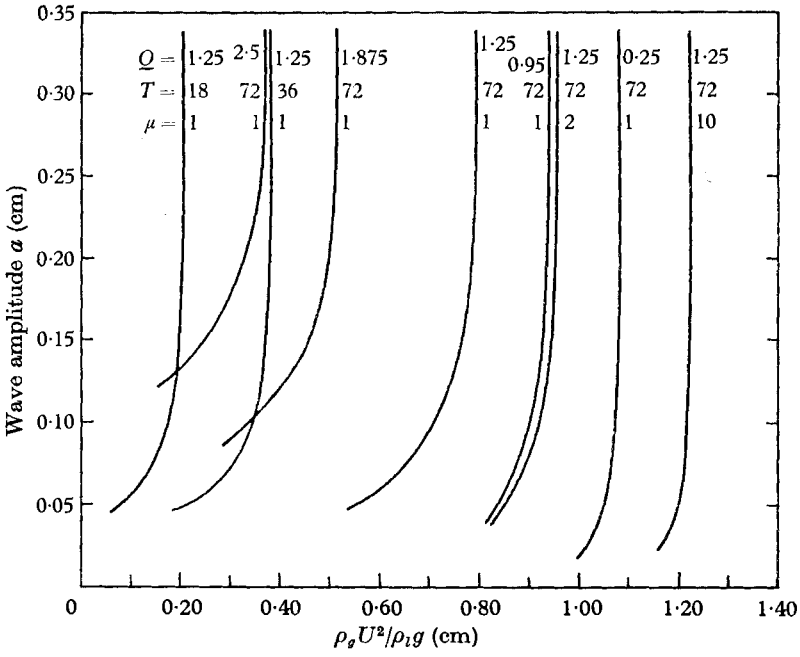

FIGURE 6. Theoretical wave amplitude as a function of $\rho_g U^2/\rho_l g$ for varying liquid flow, surface tension and viscosity. In all cases, $\rho_l = 1$ g/c.c.

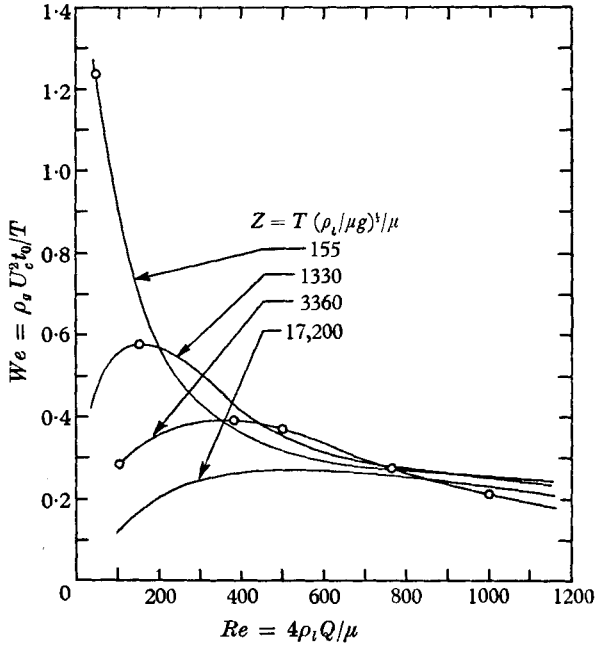

FIGURE 7. Dimensionless groups for formation of a large-amplitude wave. The circled points have been compared with experiment (see figure 8 and table 3). The symbols are defined in the summary and in the main text.

a function of $Re = 4\rho_l Q/\mu$ and $(T/\mu)(\rho_l/\mu g)^{\frac{1}{3}} = Z$ say, Z being dependent only on the liquid properties. Figure 7 shows these dimensionless groups plotted, the family of curves being obtained from computer results like those in figure 6.

The range of parameters plotted in figure 7 covers conditions for which experimental data are available, and these are shown ringed on figure 7, and are discussed in § 5. The diagram does not extend beyond $Re = 1000$ because greater values would give a turbulent liquid film. Guidance as to the values of Z was obtained from table 2 which shows the likely range for practical systems. It will be seen that figure 7 covers most of the possible cases.

Liquid	Temp. (°C)	Surface tension (dyn/cm)	Density (g/c.c.)	Viscosity (cP)	Z
60 % wt aqueous glycerol	20	67·5	1·15	10·95	135
25 % wt aqueous glycerol	20	69	1·06	2·095	1,230
Benzene	80·1 B. Pt	21·25	0·82	0·31	4,430
Acetone	56·3 B.Pt	19·05	0·75	0·24	5,420
Carbon tetrachloride	76·8 B. Pt	19·9	1·48	0·50	2,670
Water	20	72	1·0	1·0	3,360
	100 B. Pt	58·8	0·96	0·28	15,200
Molten iron	1,400	1,835	6·9	2·015	63,700
Mercury	20	465	13·55	1·55	25,800
Sodium	97·7	294	0·93	0·726	20,500
Potassium bromide (molten salt)	800	83·8	2·07	1·19	3,950

TABLE 2. Values of $Z = T(\rho_l/\mu g)^{\frac{1}{3}}/\mu$ for various liquids.

5. Flooding in wetted-wall columns

Hewitt & Wallis (1963) experimented with a $1\frac{1}{4}$ in. diameter vertical tube with a water film running down the inside wall and air blown up countercurrently through the middle. They took high-speed ciné pictures of the film and had this to say about the flooding point: 'Below the flooding point the liquid flow appeared steady and smooth and only very slightly wavy towards the bottom of the tube. Just below the flooding point an occasional sudden pulse, resembling a very large wave, would appear on the liquid film and hang there for a moment. At the flooding point this wave grew so large that the whole flow was disrupted and water was expelled from the top of the tube; at the same time the flow pattern in the whole tube became chaotic and the liquid film broke up into a series of large waves and surges.' We have quoted this passage because it describes, from experimental observations, exactly what our theory predicts, namely, the formation of a standing wave on the liquid film, the wave being stable within a very narrow range of gas flow rates. Measurements of flooding velocities in vertical tubes have been made by Verschoor (1938), Wallis (1961, 1962), Hewitt & Wallis

(1963) and Nicklin & Davidson (1962); comparisons between these data and the predictions of our theory are given in figure 8 and table 3. In applying the theory to this case of flooding in a vertical tube, the following simplifications were made.

(*a*) The total liquid flow rate was divided by the circumference of the tube, to get Q the volume flow per unit perimeter.

(*b*) No modification was made to the surface tension term in (12) to allow for the curvature of the tube wall.

(*c*) The gas velocity U was calculated from the volume flow rate of gas divided by the core area which was taken as the tube area minus the area occupied by the liquid film of thickness t_0; t_0 was calculated for a plane surface with the same value of Q.

(*d*) No allowance was made for the effect on the gas flow pattern of the finite ratio of wave amplitude to tube diameter.

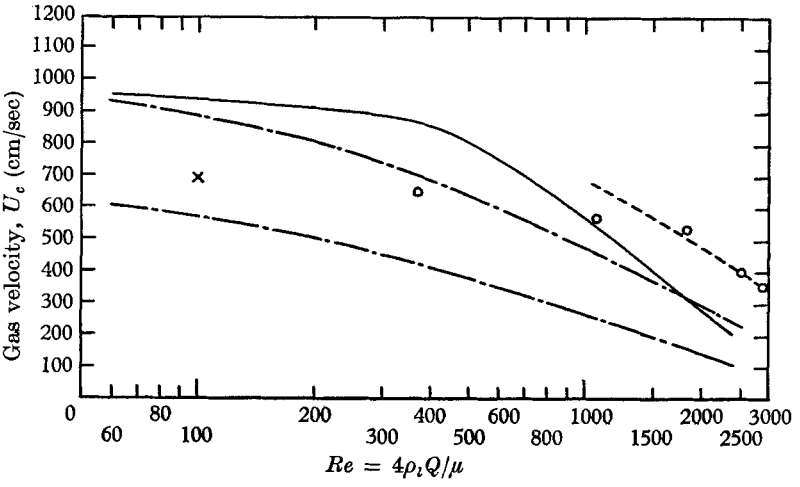

FIGURE 8. Flooding in wetted-wall columns (air-water system); comparison of experiment with the theory for the occurrence of a large-amplitude wave. ——, theory. ×, Standing-wave experiment; O, Nicklin & Davidson (1962). - — -, Wallis (1961) for a 1 in. diam. tube, his experimental data being correlated on the top and bottom curves for smooth and rough tube end connexions, respectively. – – –, Hewitt & Wallis (1963).

Figure 8 shows that, in spite of these simplifications, the theory gives reasonable agreement with the experiments. The latter show considerable scatter because of varying entrance conditions, a smooth entry giving higher flooding velocity. The mechanism of this effect is not clear, but the lower flooding velocity with rough entry conditions is presumably due to greater turbulence in the air or possibly water streams. However, the agreement between Hewitt & Wallis's (1963) data and Nicklin & Davidson's (1962) data show that, with smooth entry conditions, flooding is a reproducible phenomenon. These data and the earlier data of Wallis (1961) show that the theory gives a quite good prediction of the observed flooding velocity up to Reynolds numbers of about 1000, but above this value the liquid film may be turbulent (Binnie 1957) and this may account for the differences between theory and experiment shown at high Reynolds numbers in figure 8.

uid	Gas	Tube diameter (cm)	Liquid Reynolds number ($4Q\rho_l/\mu$)	Surface tension (dyn/cm)	Liquid viscosity (cP)	Liquid density (g/c.c.)	$\frac{Z}{T(\rho_l/\mu g)^{\frac{1}{3}}/\mu}$	Limiting gas velocity (U_c cm/sec) Theory	Expt.	Difference (%)	Inves
	Air	2·54	200	72	1	1	3360	912	800	+14	Wallis (
	Air	2·54	500	72	1	1	3360	806	635	+27	Wallis (
	Air	2·54	1000	72	1	1	3360	566	475	+19	Wallis (
enzene	Air	0·5	35	33·2	0·80	1·11	2160	764	525	+46	Verscho
ormate	Air	0·5	28	24·7	0·79	0·88	1515	679	425	+60	Verscho
queous ol	Air	1·91	136	71	4	1·08	536	912	600	+52	Wallis (
queous ol	Air	1·91	64	69	9	1·13	179	948	530	+79	Wallis (

TABLE 3. Experimental data on flooding in vertical tubes: comparison with theory. In all cases $\rho_g = 0{\cdot}00122$ g/c.c.

Table 3 shows theoretical results from figure 7, and experimental data for liquids with viscosity and surface tension different from that of water; Wallis's (1961) data for air–water with smooth entry conditions are also shown for comparison. The theory allows fairly well for the variation in physical properties.

The approximate agreement between the theory of the standing wave and the experimental flooding data suggests that the phenomena are related. But the theory of the standing wave was derived from the orifice experiment in which the standing wave is initiated and stabilized by the pressure gradients through the orifice. It is not easy to see how a standing wave can form in a wetted-wall column, particularly in view of the requirement of separation of the gas flow on the leeward side of the wave crest. Apart from Hewitt & Wallis's photographs, there is no direct evidence, and we can only speculate as to the manner in which a standing wave is initiated in a wetted-wall column; this may be as follows:

(i) At the lower end of a wetted-wall column, the pressure gradients in the gas may induce a standing wave. This instability occurs when a gas stream accelerates over a falling liquid film, and was considered by Davidson & Howkins (1957); the same authors showed further (Howkins & Davidson 1958*a*, *b*) that the resultant wave is not crucially dependent on the orifice dimensions provided the necessary pressure gradients are present.

(ii) Alternatively, it is conceivable that separation can occur on the leeward side of one of the ripples which are always present on the surface of the liquid film except at very low liquid Reynolds numbers. Separation of the airflow from such ripples is not a very probable event, but on the other hand there are at any instant many ripples in a wetted-wall column; if the airflow is enough to support a standing wave, only one ripple needs to have separated air flow for a very short time to give a standing wave. A probability argument of this kind is in line with the paragraph quoted above from Hewitt & Wallis's paper describing 'an occasional pulse'. On this argument it seems unlikely that the airflow can exceed the flow for the formation of a standing wave *without* such a wave being actually formed.

The points in figure 7 corresponding to the theoretical results in table 3 have been circled to show which regions of figure 7 have been verified experimentally. Clearly, more data are required before figure 7 can be used with complete confidence, but it should be valuable to the designer of wetted-wall columns as a guide for calculating flooding velocities.

The dimensionless groups in figure 7 may be compared with those used by Wallis (1961, 1962) who correlated $V_g \rho_g^{\frac{1}{2}} [gD(\rho_l - \rho_g)]^{-\frac{1}{2}}$ with $V_f \rho^{\frac{1}{2}} [gD(\rho_l - \rho_g)]^{-\frac{1}{2}}$ where V_g and V_f are the superficial velocities (volume flow rate divided by the cross-sectional area of the tube) of both phases, and D is the tube diameter. It is particularly interesting to note that the tube diameter does not appear in the groups in figure 7. This absence of D agrees with the results of Verschoor (1938) who found that U_c is independent of D, unless D is very small; with very small values of D, the circularity effect, (*b*) above, must be important.

One of us (C. J. S.) would like to acknowledge the support given by a Sir James Caird Scholarship.

REFERENCES

BINNIE, A. M. 1957 *J. Fluid Mech.* **2**, 551.

DAVIDSON, J. F. & HOWKINS, J. E. 1957 *Proc. Roy. Soc.* A, **240**, 29.

HEWITT, G. F. & WALLIS, G. B. 1963 Multi-phase Flow Symposium, p. 62. *A.S.M.E.* Meeting at Philadelphia.

HOWKINS, J. E. & DAVIDSON, J. F. 1958*a* *A.I.Ch.E. J.* **4**, 324.

HOWKINS, J. E. & DAVIDSON, J. F. 1958*b* *Chem. Eng. Sci.* **7**, 235.

JEFFREYS, H. & JEFFREYS, B. S. 1946 *Methods of Mathematical Physics*, p. 266. Cambridge University Press.

LAMB, SIR HORACE 1932 *Hydrodynamics*, 6th ed., p. 373. Cambridge University Press.

NICKLIN, D. J. & DAVIDSON, J. F. 1962 *Proceedings of the Symposium on Two-Phase Fluid Flow*, p. 29. Inst. Mech. Engrs, London.

URSELL, F. 1956 *Surveys in Mechanics*, p. 216 (ed. by G. K. Batchelor & R. M. Davies). Cambridge University Press.

VERSCHOOR, H. 1938 *Trans. Inst. Chem. Engrs*, **16**, 66.

WALLIS, G. B. 1961 *A.E.E.W.* –R 123, H.M.S.O.

WALLIS, G. B. 1962 General Engineering Laboratory, Schenectady, New York, 62 GL 132.